

# An Efficient Gradient Sensitive Alternate Framework for Variational Quantum Eigensolver with Variable Ansatz

Ze-Tong Li<sup>1,3,4</sup>, Fan-Xu Meng<sup>2,3,4</sup>, Han Zeng<sup>2,3,4</sup>, Zai-Chen Zhang<sup>2,3,4,5</sup>, and Xu-Tao Yu<sup>1,3,4,5</sup>

<sup>1</sup>State Key Laboratory of Millimeter Waves, Southeast University, Nanjing 210096, China

<sup>2</sup>National Mobile Communications Research Laboratory, Southeast University, Nanjing 210096, China.

<sup>3</sup>Frontiers Science Center for Mobile Information Communication and Security, Southeast University, Nanjing 210096, China.

<sup>4</sup>Quantum Information Center, Southeast University, Nanjing 210096, China.

<sup>5</sup>Purple Mountain Lab, Nanjing 211111, China.

Variational quantum eigensolver (VQE), aiming at determining the ground state energy of a quantum system described by a Hamiltonian on noisy intermediate-scale quantum (NISQ) devices, is among the most significant applications of variational quantum algorithms (VQAs). However, the accuracy and trainability of the current VQE algorithm are significantly influenced due to the *barren plateau* (BP), the non-negligible gate error and limited coherence time in NISQ devices. To tackle these issues, a gradient sensitive alternate framework with variable ansatz is proposed in this paper to enhance the performance of the VQE. We first propose a theoretical framework solving VA-VQE via alternately solving a gradient magnitudes related multi-objective optimization problem and the original VQE. Then, we propose a novel implementation based on the candidate tree based double  $\epsilon$ -greedy strategy and modified multi-objective genetic algorithm. As a result, the local optimum are avoided both in ansatz and parameter perspectives and the stability of output ansatz is enhanced. Furthermore, the experimental results show that, compared with the (arXiv:2010.10217) implementation, our framework is able to obtain the improvement of the error of the found solution, the quantum cost and the stability by up to 59.8%, 39.3% and 86.8%, respectively.

Fan-Xu Meng: Equal contribution to Ze-Tong Li

Xu-Tao Yu: [yuxutao@seu.edu.cn](mailto:yuxutao@seu.edu.cn)

## 1 Introduction

Quantum computing, a promising paradigm for solving many classically intractable problems [1, 2, 3, 4], is confronted with Noisy Intermediate-Scale Quantum (NISQ) era [5]. NISQ devices, characterized as small amount and short coherent time of qubits and low fidelity of quantum gates, seems difficult to efficiently apply the extraordinary quantum algorithms.

Invigoratingly, a scheme of hybrid quantum-classical algorithm kindles the hope of extracting quantum advantage of NISQ devices. In this scheme, the quantum computer maintains a parameterized quantum circuit (aka. ansatz), and the classical computer runs an optimizer to find the parameters that minimize the cost function with respect to the ansatz. This novel scheme was first proposed as variational quantum eigensolver (VQE) [6] to find the ground-state energy, and generalized for solving linear systems [7], simulating dynamics [8], decomposing matrix [9, 10], reducing dimensionality of data [11] and solving problems in data science domain [12, 13, 14]. In the following text, the term VQE is used to indicate all methods that adopt the aforementioned scheme.

The VQE have experimentally shown effectiveness towards small-scale problems [15]. The elaborately engineered ansatzes [16] with fixed layer structure and adjustable cardinality of layers have impressively exhibited high expressibility, the ability to express extensive range of quantum states. However, the performance of VQE with the ansatzes degrades significantly with respect to the increment of the qubit number and circuit depth [17]. The phenomena of the degradation

are generally exhibited as the non-ignorable absolute error between the converged cost function value and the exact minimum.

One reason to the degradation is that the VQE suffers from the so-called barren plateau [18] that the gradient magnitudes vanishes exponentially with respect to the system scale. The severity of the BP phenomenon linked to the number of entanglements [19, 20, 21, 22] and the expressibility [23]. The other reason is quantum hardware noise both in quantum gates and qubits. The influence of the noise accumulates with the number of quantum gates and the circuit depth [24], and cause the accuracy reduction of the observable estimation. This significantly impedes the convergence of the cost function since the value of cost function and its gradient are inaccurate, which is known as the noise-induced barren plateaus [24].

Recently, the variable ansatz strategy [17, 25, 26, 27, 28, 29, 30] has emerged as a promising technique to reserve the quantum advantage in the large-scale situation. Unlike the structure fixed ansatz, the layer constraint is relaxed in variable ansatz and gates can be added to anywhere in the ansatz as required. As a result, both the size and the depth of the constructed ansatz can be effectively reduced, and thus better solutions can be found. Nevertheless, implementing the VQE with variable ansatz (VA-VQE) exists a significant space overhead for the ansatz layout optimization procedure, and consequently requires substantially more computing resources than the structure fixed ansatz.

To further improve the efficiency, several techniques from intelligent algorithm have also been introduced. A kind of exact-performance based methods are proposed [25, 27, 28, 31]. In these methods, ansatzes are sampled as trail ansatzes and trained completely so that the cost function value of each trained trail ansatz reflects the exact performance of the ansatz. Benchmarking ansatzes by their exact performance achieves the precise optimal selection among trail ansatzes. However, training every sampled ansatzes completely introduces tremendous cost function determinations which is time-consuming because each determination of cost function requires substantial quantum measurements. Therefore, the range of sampled ansatzes is narrow if the quantity of quantum measurements is limited. This

may result in local optimum from the ansatz perspective.

Attempting overcoming this hurdle, several performance predictor based methods are proposed [17, 30]. These methods construct ansatzes layerwisely and maintain parameter pools from which values of parameters are exploited to calculate the cost function value as the performance predictor. Introducing the weight sharing policy [32], parameters are shared among layers with similar structures. Thus, the number of parameters in the parameter pool required to be trained is effectively reduced. These methods first train the parameter pools iteratively. In each iteration, some ansatzes are sampled based on the sampling strategy. Then, the parameters corresponding to the ansatzes are updated in specified steps (especially single step) by gradient based optimizer. After training the parameter pools, the optimal ansatz selection procedure is processed. Quantities of ansatzes are sampled and evaluated by the performance predictor. Finally, the ansatz with best performance, generally the lowest cost function value, are selected as the optimal ansatz.

This kind of methods boosts the efficiency in finding optimal ansatz by avoiding complete training of ansatzes. However, since the parameters are highly shared and the training step of each ansatz is insufficient to converge, the current cost function values may not express the actual performances of the ansatzes, and hence the output suffers from high variance. This may results from two issues. The first is the training competitions that the values of the parameters in ‘good’ ansatzes with promising layouts may be disturbed by the training of ‘bad’ ansatzes incurred by the weight sharing policy. The second issue is that the policy for ansatz layout optimization exploits the cost function value only as the benchmark to find the optimal ansatz structure. The mediocre ansatz whose cost function value is currently lowest and cannot be further decreased may be selected as the optimum. Contrarily, the promising ansatzes may be discarded because of its temporarily high cost function value.

In this paper, addressing on these issues, we propose a gradient sensitive alternate framework (GSA) for VA-VQE. The GSA alternately optimizes the structure of the ansatz and corresponding parameters via taking the gradient magnitudes into consideration. Contributions are listed

below:

- We first propose a theoretical framework solving VA-VQE via alternately solving a gradient magnitudes related multi-objective optimization problem and the original VQE, so that the local optimum can be avoid from the ansatz perspective and the stability is enhanced compared to other VA-VQE methods.
- For the initialization of parameters for the alternate optimization, we first exploit the candidate tree based double  $\epsilon$ -greedy strategy to differentiate ansatzes based on their cost function values and the gradient magnitudes in training the parameter pool, so that the training competitions are mitigated and the local optimal can be evaded from the parameter perspective.
- We further reduce the size of search space of the ansatz via applying gate commutation rules and establishing a bijection between the search space and the practical implementations of ansatzes to boost the time efficiency of the optimal ansatz and parameter determination.
- We adopt relatively fair criteria for measuring the performance of VA-VQE, so that the transverse comparison among methods of VA-VQE can be clearly conducted. As a result, the GSA shows conspicuously better performance in average compared to the structure fixed HEA up to 87.9% improvement in terms of absolute error, and to the VA-VQE method QAS [17] up to 59.8%, 39.3% and 86.8% improvement in terms of absolute error, quantum cost (the number of calculations of cost function) and stability (mean square error), respectively.

This paper are structured as following: In Sec.2, we briefly introduce the basic knowledge. Then, the gradient sensitive theoretical framework based on the alternate optimization are proposed in Sec.3. The detail of practical implementation of GSA is proposed in Sec.4. Subsequently, we conduct numerical simulations with relatively fair criteria in Sec.5 to show the advantages of our proposed method. Finally, we conclude this work in Sec.6. Notice that the examples and

pseudocodes of algorithms are summarized in Appendix A and E, respectively.

## 2 Background

### 2.1 Variational Quantum Eigensolver

In this work, we address the variational quantum eigensolver (VQE) tasks identified by sets of tuples  $\mathbb{T} = \{(O_i, \rho_i, f_i)\}$  aiming at minimizing a cost function

$$C(\theta) = \sum_i f_i(\text{Tr}[O_i U(\theta) \rho_i U^\dagger(\theta)]), \quad (1)$$

where  $\{\rho_i\}$  is the training set formed as n-qubit quantum states,  $U(\theta)$  is a specified parameterized quantum circuit (aka. ansatz) with parameters  $\theta$ ,  $O_i$  are observables and  $f_i$  are bounded second-order differentiable functions that encode the problem with respect to the operand observable  $O_i$  and state  $\rho_i$ . Generally, while implementing the VQE, the quantum computer applies the ansatz  $U(\theta)$  and processes the quantum measurements to determine expectations  $\text{Tr}[O_i U(\theta) \rho_i U^\dagger(\theta)], \forall i$ . The classical computer computes the cost function value and runs an optimization algorithm to find the optimal parameters  $\theta^*$  that minimize the cost function. We provide an example finding the ground state energy of a quantum system described by a Hamiltonian in Eg.1.

### 2.2 Quantum Gradient

In the optimization procedure of large scale VQE, the gradient-based methods (e.g., gradient descent) are generally more preferred than gradient-free methods (e.g., Nelder-Mead) [33]. In the gradient-based methods, the gradient of the cost function with respect to the parameters is essentially estimated in each optimization iteration.

Without loss of generality, an ansatz can be mathematically defined by

$$U(\theta) := \prod_{l=1}^{N_l} U_l(\theta_l) W_l, \quad (2)$$

where  $U_l(\theta_l) = \exp(-i\theta_l V_l)$ ,  $V_l$  is a Hermitian operator,  $W_l$  is a non-parametrized quantum gate. Then, the partial derivative of an expectation  $E(\theta) = \text{Tr}(OU(\theta)\rho U^\dagger(\theta))$  with respect to the

$k$ th parameter  $\theta_k$  is

$$\begin{aligned}\partial_k E(\boldsymbol{\theta}) &\equiv \frac{\partial E(\boldsymbol{\theta})}{\partial \theta_k} \\ &= i\text{Tr} \left( \left[ V_k, U_L^\dagger O U_L \right] U_R \rho U_R^\dagger \right),\end{aligned}\quad (3)$$

where we use the notations

$$U_R \equiv \prod_{l=1}^{k-1} U_l(\theta_l) W_l, \quad (4)$$

$$U_L \equiv \prod_{l=k}^{N_L} U_l(\theta_l) W_l. \quad (5)$$

In this paper, we apply the parameter-shift rule [33] for the gradient estimating. We assume that all parameterized quantum gates are Pauli rotations. Therefore, the partial derivative of  $E(\boldsymbol{\theta})$  with respect to  $\theta_k$  is

$$\partial_k E(\boldsymbol{\theta}) = \frac{1}{2} \left[ E(\boldsymbol{\theta} + \frac{\pi}{2} \mathbf{e}_k) - E(\boldsymbol{\theta} - \frac{\pi}{2} \mathbf{e}_k) \right], \quad (6)$$

where  $\mathbf{e}_k$  is a vector whose  $k$ th element is 1 and others are 0.

### 2.3 Gradient Decent

Gradient decent is literately a gradient based optimizer which has been generally used in training VQE [7, 8, 11, 12]. The kernel process of the gradient decent can be mathematically represented as

$$\boldsymbol{\theta} \leftarrow \boldsymbol{\theta} - \alpha \nabla C(\boldsymbol{\theta}), \quad (7)$$

where  $\alpha$  is the step size.

In this paper, we exploit a line search to estimate the step size  $\alpha$  instead of a fixed one. In each optimization step,  $\alpha$  satisfies the Wolfe conditions [34]

$$C(\boldsymbol{\theta} - \alpha \mathbf{g}) \leq C(\boldsymbol{\theta}) - c_1 \alpha \|\mathbf{g}\|_2^2, \quad (8)$$

$$\nabla C(\boldsymbol{\theta} - \alpha \mathbf{g})^T \mathbf{g} \geq c_2 \|\mathbf{g}\|_2^2, \quad (9)$$

where  $\mathbf{g} = \nabla C(\boldsymbol{\theta})$ ,  $0 < c_1 < c_2 < 1$ . To facilitate the  $\alpha$  determination, given a reference step size  $\alpha_0$ , we gradually decrease  $\alpha$  from  $\alpha_0$  by repeating  $\alpha \leftarrow \rho \alpha$  until Eq.(8) establishing, where  $\rho < 0$ . In this paper, we empirically set  $c_1 = 10^{-4}$  and  $\rho = 0.618$ .

### 2.4 Expressibility

In the absence of prior knowledge about solution unitaries  $\mathbb{U}_s$  of a VQE task, the ability of ansatz to generate large range of unitaries  $\mathbb{U}$  to guarantee  $\mathbb{U}_s \cap \mathbb{U} \neq \emptyset$  is required. The expressibility of an ansatz describes the degree to which it uniformly explores the unitary group  $\mathcal{U}(2^n)$ , and can be simply considered as the range of unitaries the ansatz can generate. By comparing the uniform distribution of unitaries obtained from  $\mathbb{U}$  to the Haar distribution of unitaries from  $\mathcal{U}$ , the expressibility of an ansatz can be defined by the superoperator [35, 36]:

$$\begin{aligned}\mathcal{A}_u^{(t)} &:= \int_{\mathcal{U}(2^n)} d\mu(V) V^{\otimes t}(\cdot)(V^\dagger)^{\otimes t} \\ &\quad - \int_{\mathbb{U}} dU U^{\otimes t}(\cdot)(U^\dagger)^{\otimes t},\end{aligned}\quad (10)$$

where  $d\mu(V)$  is the volume element of the Haar measure and  $dU$  is the volume element corresponding to the uniform distribution over  $\mathbb{U}$ . Here we are especially interested in the expressibility of the ansatz with respect to the input quantum state  $\rho$  and the observable  $O$

$$\epsilon_{\mathbb{U}}^\rho := \left\| \mathcal{A}_{\mathbb{U}}^{(2)}(\rho^{\otimes 2}) \right\|_2, \quad (11)$$

$$\epsilon_{\mathbb{U}}^O := \left\| \mathcal{A}_{\mathbb{U}}^{(2)}(O^{\otimes 2}) \right\|_2. \quad (12)$$

Small values of  $\epsilon_{\mathbb{U}}^\rho$  and  $\epsilon_{\mathbb{U}}^O$  indicate the high expressibility of the ansatz.

### 2.5 Barren Plateau and Trainability

As one of the key challenges of VQE, the barren plateau phenomenon exhibited the exponentially decreasing of the gradient magnitudes with respect to the system size  $n$  [18], and was generalize that the ansatzes' expressibility [23] and the amount of entanglement [19, 20, 21, 22] play significant roles in leading to barren plateaus. We highlight the severity of BP phenomenon with respect to  $n$  and the expressibility of the ansatz by the limited variance of gradient magnitudes

$$\text{Var}[\partial_k C(\boldsymbol{\theta})] \leq \frac{g(\rho, O, U)}{2^{2n} - 1} + f(\epsilon_{\mathbb{U}_L}^O, \epsilon_{\mathbb{U}_L}^\rho), \quad (13)$$

where  $g(\rho, O, U)$  is the prefactor in  $O(2^n)$ ,

$$f(x, t) = 4xy + \frac{2^{n+2} \left( x \|O\|_2^2 + y \|\rho\|_2^2 \right)}{2^{2n} - 1}, \quad (14)$$

and  $\mathbb{U}_L$  and  $\mathbb{U}_R$  are ensembles of  $U_L$  and  $U_R$ , respectively [23]. The first term on the right in Eq.(13) indicate the variance of 2-design ansatz and is in  $O(1/2^n)$ , and the second term is the expressibility-dependent correction. From the Chebyshev's inequality, the trainability of an ansatz can be described by

$$\Pr[|\partial_k C(\boldsymbol{\theta})| \geq \delta] \leq \frac{\text{Var}[\partial_k C(\boldsymbol{\theta})]}{\delta^2}, \forall \delta > 0. \quad (15)$$

When the ansatz exhibits the BP phenomenon, the probability decreases exponentially with respect to  $n$ , which indicate that the precision to determine a cost minimizing direction is exponentially large to  $n$  [28, 37, 38]. It is remarkable that ansatz with higher expressibility suffers lower trainability since it exhibit more severe BP phenomenon.

Here we remark that there exist an another kind of barren plateaus, the noise-induced barren plateaus [24], caused by the imperfect quantum hardware. The cost function value concentrates exponentially around its average as the influence of noise accumulates, since the noise models acting throughout the ansatz maps the input state toward the fixed point of the noise model [24, 39].

This challenging phenomenon cannot simply be escaped by changing the optimizer [38]. While several attempts have been made to mitigate the severity of the barren plateau [40, 41, 42, 43, 44], it is widely accepted that the variable ansatz strategy is promising to address this issue via automatically balancing the expressibility, the influence of noise and the trainability.

## 2.6 Hardware Constraints

Generally, only a limited number of gates are available on a practical quantum computer and the two-qubit gates are only allowed to be applied on a specific set of qubit pairs. These available gates are known as native gates of the quantum hardware. In this paper, we assume the native gates on a  $n$ -qubit quantum system to be  $R_y$ ,  $R_z$  and CNOT mathematically represented as

$$R_y^q(\theta) = e^{-i\frac{\theta}{2}\sigma_y} = \begin{bmatrix} \cos\frac{\theta}{2} & -\sin\frac{\theta}{2} \\ \sin\frac{\theta}{2} & \cos\frac{\theta}{2} \end{bmatrix}, \quad (16)$$

$$R_z^q(\theta) = e^{-i\frac{\theta}{2}\sigma_z} = \begin{bmatrix} e^{-i\theta/2} & 0 \\ 0 & e^{i\theta/2} \end{bmatrix}, \quad (17)$$

$$\begin{aligned} \text{CNOT}^{q_a, q_b} &= |0\rangle\langle 0|^{q_a} \otimes I^{q_b} \\ &+ |1\rangle\langle 1|^{q_a} \otimes X^{q_b} \end{aligned} \quad (18)$$

where superscript  $q, q_a, q_b$  indicate the qubits on which the quantum gates act,  $\sigma_y$  and  $\sigma_z$  are Pauli operators mathematically represented as

$$\sigma_y = \begin{bmatrix} 0 & -i \\ i & 0 \end{bmatrix}, \sigma_z = \begin{bmatrix} -1 & 0 \\ 0 & 1 \end{bmatrix}, \quad (19)$$

$I$  is the identity quantum operation and  $X$  is quantum *not* gate mathematically represented as

$$I = \begin{bmatrix} 1 & 0 \\ 0 & 1 \end{bmatrix}, X = \begin{bmatrix} 0 & 1 \\ 1 & 0 \end{bmatrix}. \quad (20)$$

Moreover,  $R_z^q$  and  $R_y^q$  can be applied for all  $q \in \{1, 2, \dots, n\}$ , while CNOT gates  $\text{CNOT}^{q_a, q_b}$  are unidirectional available on adjacent qubit pairs, i.e.,  $q_b = (q_a + 1) \bmod n$ . Note that the proposed framework can be easily adjusted for different native gate sets.

## 3 Theoretical Framework

In this section, we introduce the theoretical framework derived from the problem of VQE. Then, we equivalently transform the solving procedure into solving a series of gradient magnitudes related multi-objective optimization problem.

Recall that a VQE task can be considered as minimizing a cost function, which is summarized in Prob.1.

**Problem 1 (VQE).** *Given an ansatz  $U(\boldsymbol{\theta})$  and a task  $\mathbb{T}$ , the problem of VQE is to find parameters that minimize the cost function  $C(\boldsymbol{\theta})$ , i.e.,*

$$\min_{\boldsymbol{\theta} \in \mathbb{D}^{N_p}} C(\boldsymbol{\theta}) = \sum_i f_i(\text{Tr}[O_i U(\boldsymbol{\theta}) \rho_i U^\dagger(\boldsymbol{\theta})]), \quad (21)$$

where  $\mathbb{D} \subset \mathbb{R}$ ,  $N_p$  is the cardinality of trainable parameters in  $U$ .

While introducing the VA-VQE framework as summarized in Prob.2, the structure of ansatz  $U$  is treated as a variable that need to be optimized in the cost function, i.e.,

$$C(U, \boldsymbol{\theta}) = \sum_i f_i(\text{Tr}[O_i U(\boldsymbol{\theta}) \rho_i U^\dagger(\boldsymbol{\theta})]). \quad (22)$$

**Problem 2 (VA-VQE).** *Given a search space of ansatzes  $\mathbb{S}$  and a task  $\mathbb{T}$ , the problem of VA-VQE is to find ansatzes and corresponding parameters that minimize the cost function  $C(U, \boldsymbol{\theta})$*

$$\min_{U \in \mathbb{S}, \boldsymbol{\theta} \in \mathbb{D}^{N_p}} C(U, \boldsymbol{\theta}), \quad (23)$$



where  $C(U, \theta)$  forms as Eq.(22),  $\mathbb{D} \subset \mathbb{R}$ ,  $N_p$  is the cardinality of trainable parameters in  $U$ .

Practically, the VA-VQE methods automatically construct ansatzes by quantum gates from a given gate set  $\mathbb{G}$ , i.e.  $\mathbb{S} = \mathbb{G}^\infty$ , and find ones with trained parameters that minimize the cost function. The search space of ansatz actually scales infinitely since the depth of ansatz circuits can be infinitely large. However, the trainability of the ansatz is substantially limited by the number of quantum gates because the expressibility and the impact of noise of the ansatz may increase with respect to the number of quantum gates, which aggravates the BP phenomenon. On the other hand, it is intractable to search solutions with enormous (even infinite) search space of ansatz. Therefore, a fixed or gradually increased maximum number  $n_g$  of quantum gates is introduced as  $\mathbb{S} = \mathbb{G}^{N_g}$ , where  $N_g$  is sufficiently large that  $\exists U \in \mathbb{G}^{N_g}$  such that  $\mathbb{U} \cap \mathbb{U}_s \neq \emptyset$ . Nevertheless, determining exact solutions requires solving combinatorial optimization in exponentially large search space, which conceals the efficiency of VQE. Most of methods [17, 26, 28, 30, 31] attempt to provide approximate solutions in polynomial complexity with respect to  $g$ . Although the gradient is generally estimated for the optimization of parameters, its magnitude are neglected to provide a guideline for the optimization of structure of ansatz. Therefore, several undesirable phenomena listed below may occurred:

1. The ansatz which exhibits severe barren plateau, and thus the gradient magnitude is highly close to 0, is selected to test the cost function value multiple times.
2. The trivial ansatz whose parameters are completely trained, i.e. the gradient magnitude is highly close to 0, is selected as the optimal ansatz, since it temporarily cost less than potentially better ansatz with incompletely trained parameters, i.e. the gradient magnitude is significantly larger than 0.

These phenomena result in the local optimal of the VA-VQE from the ansatz perspective and instability of optimal ansatz and cost function value outputs.

Here we first introduce the gradient magnitude in solving VA-VQE problem to explicitly supervise the severity of BP phenomenon and the

completeness of parameter training of ansatzes. We define a subproblem the gradient related ansatz multi-objective optimization (GRAMO) in Prob.3.

**Problem 3 (GRAMO).** *Given a search space of ansatzes  $\mathbb{S}$ , a task  $\mathbb{T}$  and a set of parameters  $\mathbb{P}$  such that  $\exists! \theta_U \in \mathbb{P}$ ,  $\forall U \in \mathbb{S}$ , the problem of GRAMO is to find ansatzes that minimize the cost function  $C(U, \theta_U)$  and maximize the gradient magnitude of the cost function, i.e.,*

$$\min_{U \in \mathbb{S}} C(U, \theta_U), \max_{U \in \mathbb{S}} \frac{\|\nabla C(U, \theta_U)\|_2}{|\theta_U|} \quad (24)$$

where  $C(U, \theta_U)$  forms as Eq.(22),  $\nabla C(U, \theta_U)$  is the gradient of  $C(U, \theta_U)$  with respect to  $\theta_U$ ,  $\theta_U \in \mathbb{P}$  and  $|\theta_U|$  is the cardinality of parameters in  $\theta_U$ .

The (1-rank) solution of Prob.3 is defined as the non-dominated set  $\mathbb{U}_n$  consisting of all  $U$  such that no  $V \in \mathbb{S}$  simultaneously establishes inequalities

$$C(V, \theta_V) < C(U, \theta_U), \quad (25)$$

$$\frac{\|\nabla C(V, \theta_V)\|_2}{|\theta_V|} \geq \frac{\|\nabla C(U, \theta_U)\|_2}{|\theta_U|}. \quad (26)$$

As a result, structures of ansatzes with low cost function values or large gradient magnitudes, in other word, high absolute performance or high potentiality, are selected as solutions. Furthermore, the  $k$ -rank solution  $\mathbb{U}_n(k)$  of the problem is defined by  $\mathbb{U}_n(k) := \mathbb{U}_n(k-1) \cap \mathbb{U}'_n$ , where  $\mathbb{U}'_n$  is the 1-rank solution of Prob.3 with search space  $\mathbb{S} \setminus \mathbb{U}_n^{k-1}$ .

We solve the VA-VQE problem by alternately solving Prob.1 and Prob.3 as summarized in Alg.1. When the gate set  $\mathbb{G}$  and the set of problem-related tuples  $\{(O_i, \rho_i, f_i)\}$  is specified, for any initialization of  $\mathbb{P}$ , the VA-VQE can be solved iteratively. At each iteration, the non-dominated set  $\mathbb{U}_n$  is determined by solving Prob.3 the GRAMO with  $\mathbb{P}$ . Then, the optimal parameters  $\theta_U \in \mathbb{P}$  are updated via solving Prob.1 the VQE,  $\forall U \in \mathbb{U}_n$ . The alternate optimization procedure terminates until  $\mathbb{U}_n$  and  $\mathbb{P}$  are converged.

**Theorem 1 (Convergence).**  *$\mathbb{U}_n$  and  $\mathbb{P}$  in Alg.1 converges such that  $\forall (U \in \mathbb{U}_n, \theta_U \in \mathbb{P})$  are solutions of Prob.2 for all  $\mathbb{P}_0$  satisfied that  $\exists V \in \mathbb{G}^\infty$  such that*

$$\exists \theta^*, C(V, \theta^*) = \min_{U, \theta} C(U, \theta), \quad (27)$$

$$\forall \delta > 0, C(V, \theta_V \in \mathbb{P}_0) \neq \max_{\theta \in \Theta_{V, \delta}} C(V, \theta), \quad (28)$$

where

$$\Theta_{V,\delta} = \{\theta \mid \|\theta - \theta_V\|_2 < \delta\}. \quad (29)$$

The theoretical framework ends with Theorem 1 (c.f. Appendix C for the proof), which indicates that solutions of VA-VQE can be determined by Alg.1.

## 4 Solving VQE Tasks with Gradient Sensitive Variable Ansatz

In this section, the gradient sensitive alternate framework (GSA) for VA-VQE is proposed in detail. As the VA-VQE problem described, GSA takes the gate set  $\mathbb{G}$  and a set of task relative tuples  $\{(O_i, \rho_i, f_i)\}$  as inputs. Based on the gate commutation rules, the search space of ansatz  $\mathbb{S}(N_l)$  under the maximum number of layers  $N_l$  is reduced to boost the time efficiency of the optimal ansatz and parameters determination. Then, the quasi-optimal ansatz and corresponding trained parameters are output through three stages: *pool training*, *alternate training* and *VQE retraining*. In the stage of *pool training*, a candidate tree  $T$  is constructed for double  $\epsilon$ -greedy sampling and a parameter pool in which parameters are shared among ansatzes with similar structures is trained via exploiting candidate tree based double  $\epsilon$ -greedy strategy. As a result, a reasonable set of parameters  $\mathbb{P}_0$  is generated as the initialization of parameters for the next stage. Based on the multi-objective genetic algorithm, the *alternate training* applies the framework described in Alg.1 to solve the VA-VQE problem via alternately solving the GRAMO in Prob.3 and the VQE in Prob.1. Since the evolutionary algorithm is applied, the output ansatz is quasi-optimal and corresponding parameters may be incompletely trained. Therefore, the third stage *optimal ansatz retraining* is required to guarantee the completion of parameter training of the quasi-optimal ansatz. We summarize the GSA as Alg.2.

Besides, there are several parameters needed to be defined before actual running. For the entire proposed framework, they are, respectively, the maximum number of layers  $N_l$ , the reference step size  $\alpha_0$ , the convergence threshold  $\xi$ , the probability of greedy selection applying the double  $\epsilon$ -greedy strategy  $\epsilon_1$  and  $\epsilon_2$ . In the *parameter pool training*, they are, respectively, the number of sampled ansatzes  $N_{s1}$ , the maximum number

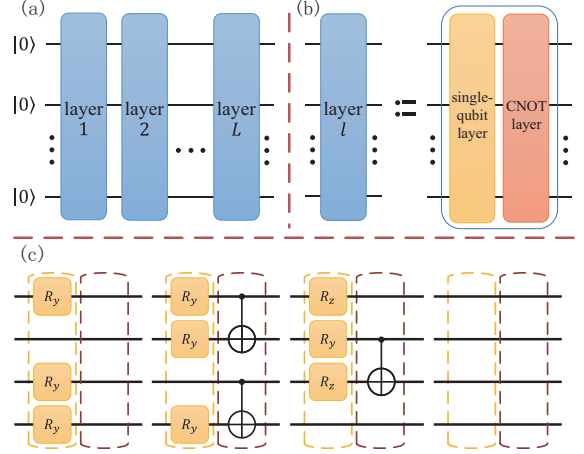


Figure 1: The layer-by-layer ansatz (a) with each layer being decomposed into two sublayers, i.e., a single-qubit gate layer and a CNOT layer; and (c) four exemplary constructions of layers.

of ranks of ansatzes whose corresponding parameters are updated  $N_{r1}$ , the stable threshold for terminating the main process  $N_{t1}$ , the maximum iteration times in the prethermalization  $N_{i0}$  and the main process  $N_{i1}$ . In the *alternate training*, they are, respectively, the population size  $N_{s2}$ , the maximum number of ranks of ansatzes whose corresponding parameters are updated  $N_{r2}$ , the stable threshold  $N_{t2}$ , the optimization step in a generation  $N_o$ , the maximum iteration times  $N_{i2}$ . In the *optimal ansatz retraining*, they include the maximum iteration times  $N_{i3}$ .

This section is organized as following: In Sec.4.1, we concretely propose the structure of search space of ansatz for the GSA, and conduct the size reduction to the search space based on the gate commutation rules. Subsequently, the *pool training*, *alternate training* and *VQE retraining* stages are explained in Sec.4.2, 4.3 and 4.4, respectively.

### 4.1 Search Space of Ansatz

Without violation of Eq.2, we compose an ansatz by a layer-by-layer fashion as shown in Fig.1. To be specific, each layer consists of a set of native disjoint single-qubit gates followed by a set of hardware-compliant disjoint CNOT gates. It can be easily derived that the number of all possible structures  $N_s$  of a layer is exponentially large with respect to the number of qubits  $n$ . We use the term state denoted by  $\mathbf{s}_j$  to indicate the  $j$ th structure is used. Then, an ansatz can be identi-

fied by a tuple of states

$$(\mathbf{s}^1, \mathbf{s}^2, \dots, \mathbf{s}^{N_l}),$$

where  $\mathbf{s}^l \in S := \{\mathbf{s}_1, \mathbf{s}_2, \dots, \mathbf{s}_{N_s}\}$ . As a result, the search space of ansatz  $\mathbb{S}(N_l)$  can be specifically represented by a tree with  $N_l+1$  layers (from layer 0 to  $N_l$ ). A node at the layer  $l > 0$  in the tree is uniquely identified by its parent node and the state, i.e.,  $\mathbf{v}^l := (\mathbf{v}^{l-1}, \mathbf{s}^l)$ , and linked to its child nodes. In the layer 0, the root node of the tree is defined with no parent node and the state  $\mathbf{s}^0$  in which no layer information is stored. Furthermore, we call the nodes in the layer  $N_l$  linked to no child nodes the leaf nodes. Finally, a path from the root node to a leaf node  $(\mathbf{v}^0, \mathbf{v}^1, \dots, \mathbf{v}^{N_l})$  represents an ansatz  $(\mathbf{s}^1, \mathbf{s}^2, \dots, \mathbf{s}^{N_l})$ .

The unrefined  $\mathbb{S}(N_l)$  is intuitively a full  $N_s$ -ary tree with  $(N_s)^{N_l}$  leaf nodes. However, this simple-mined construction can not establish the bijection between practical implementations of ansatzes and paths (c.f. Eg.2). Moreover, gates in distinct layers may deletable or mergeable (c.f. Eg.3). To further eliminate the redundant ansatzes and improve the efficiency, the paths violating the following cross-layer constraints based on gate commutation rules will be pruned.

**Constraints:** For node  $\mathbf{v}^l := (\mathbf{v}^{l-1}, \mathbf{s}^l)$  in the path  $(\mathbf{v}^0, \mathbf{v}^1, \dots, \mathbf{v}^l)$ :

1.  $R_z^q, CNOT^{q,q'} \notin \mathbf{s}^l$ , if  $R_y^q, CNOT^{q'',q} \notin \mathbf{s}^k$ ,  $\forall q$  with  $|0\rangle$  initialization,  $q'$  and  $q''$ ,  $l > k > 0$ ;
2.  $CNOT^{q_1,q_2} \notin \mathbf{s}^l$ , if  $\exists CNOT^{q_1,q_2} \in \mathbf{s}^k$ , such that  $R_y^{q_1}, R_y^{q_2}, R_z^{q_2}, CNOT^{q',q_1}, CNOT^{q_2,q'}, CNOT^{q',q_2} \notin \mathbf{s}^m$ ,  $\forall q, q', k < m < l < 0$ ;
3.  $R_z^q \notin \mathbf{s}^l$ , if  $R_y^q, CNOT^{q',q} \notin \mathbf{s}^{l-1}$ ,  $\forall q, q', l > 0$ ;
4.  $R_y^q \notin \mathbf{s}^l$ , if  $R_z^q, CNOT^{q,q'}, CNOT^{q',q} \notin \mathbf{s}^{l-1}$ ,  $\forall q, q', l > 1$ .
5.  $\mathbf{s}^l$  is empty if  $\mathbf{s}^{l-1}$  is empty,  $l > 1$ .

The first constraint follows the fact that  $R_z^q$  and  $CNOT^{q,q'}$  preserve the state of quantum system when the quantum state of  $q$  is  $|0\rangle$ . The second constraint avoids two consecutive CNOT gates with identical control and target qubits. As a result, the first two constraints eliminate deletable

combinations of quantum gates. The mergeable combinations are extinguished by constraints 3 and 4 by prohibiting consecutive  $R_z$  and  $R_y$ , respectively. Finally, the bijection between practical implementations of ansatzes and paths are established by the conjunction of constraints 3, 4 and 5. Consequently, the size of the search space  $|\mathbb{S}(N_l)|$  is significantly reduced. We provide an example the Eg.4 to demonstrate the efficiency obtained from our constraints.

## 4.2 Pool training

In this subsection, the *pool training* stage is presented in detail. Based on the weight sharing strategy, the number of parameters required to be trained are reduced to  $\mathcal{O}(N_l)$ . Moreover, the double  $\epsilon$ -greedy strategy is exploited accompanied with candidate tree to mitigate the training competitions among ansatzes. We treat the *pool training* as a one-shot training program. At each iteration, a number of ansatzes are randomly sampled and estimated. According to the estimated performance, several temporarily outstanding ansatzes are selected to update parameters in specified steps (typically one step) via gradient based optimizer.

Recall that solving VQ-VQE in the framework as described in Alg.1 requires the initialization of  $\mathbb{P}_0$  in which each structure of ansatz links to an independent set of parameters. Intuitively, that parameters  $\theta_U \in \mathbb{P}_0$  substantially reflect the actual performance of ansatz  $U$ , i.e.,  $\theta_U \approx \arg \min_{\theta} C(U, \theta)$ , facilitates the optimal ansatz determination. Therefore, we conduct a pre-training of parameters before the alternate optimization solving VA-VQE instead of random initialization. Unfortunately, the size of  $\mathbb{P}_0$  is exponentially large with respect to  $n$  and  $N_l$  result from the exponentially large  $\mathbb{S}(N_l)$ . It is impractical to adequately train  $\mathbb{P}_0$  efficiently.

Instead, we construct a parameter pool with linear size with respect to  $N_l$  via applying weight sharing strategy, and train the pool to eventually derive  $\mathbb{P}_0$ . The parameter pool can be matrix-like defined as

$$P := \begin{bmatrix} \theta_{\mathbf{s}_1,1} & \theta_{\mathbf{s}_1,2} & \dots & \theta_{\mathbf{s}_1,N_l} \\ \theta_{\mathbf{s}_2,1} & \theta_{\mathbf{s}_2,2} & \dots & \theta_{\mathbf{s}_2,N_l} \\ \vdots & \vdots & \ddots & \vdots \\ \theta_{\mathbf{s}_{N_s},1} & \theta_{\mathbf{s}_{N_s},2} & \dots & \theta_{\mathbf{s}_{N_s},N_l} \end{bmatrix}, \quad (30)$$

where  $\theta_{k,l}$  represents the parameters at  $l$ th layer



corresponding to the state  $\mathbf{s}_k$ . Then, parameters of an ansatz  $(\mathbf{v}^0, \mathbf{v}^1, \dots, \mathbf{v}^{N_l})$  is

$$\boldsymbol{\theta} := \boldsymbol{\theta}_{\mathbf{s}^1,1} \oplus \boldsymbol{\theta}_{\mathbf{s}^2,2} \oplus \dots \oplus \boldsymbol{\theta}_{\mathbf{s}^{N_l},N_l}, \quad (31)$$

where  $\oplus$  indicate the direct sum such that

$$\begin{bmatrix} a_1 \\ a_2 \\ \vdots \\ a_N \end{bmatrix} \oplus \begin{bmatrix} b_1 \\ b_2 \\ \vdots \\ b_N \end{bmatrix} = \begin{bmatrix} a_1 \\ \vdots \\ a_N \\ b_1 \\ \vdots \\ b_N \end{bmatrix}.$$

It can be simply derived that parameters in identical layer and state are shared among ansatzes, which is the direct affect of applying weight sharing strategy. Obviously, the number of trainable parameters is in  $\mathcal{O}(N_s N_l)$ , which is linear with respect to  $N_l$ . The exponentially reduction significantly boosts the efficiency of parameter training. However, the training competitions are therefore introduced.

Inspired by  $\epsilon$ -greedy strategy from traditional machine learning [45], we propose a candidate tree based double  $\epsilon$ -greedy strategy to mitigate the training competitions. Remarkably, our proposed method not only differentiate ‘good’ and ‘bad’ ansatzes, but also ansatzes among ‘good’ and ‘bad’ ansatzes.

Recall that the search space  $\mathbb{S}(N_l)$  can be represented by a tree. It is intuitive that constructing a tree to save potentially ‘good’ ansatzes and discarding potentially ‘bad’ ansatzes are reasonable for the differentiation. The tree spanned by paths representing potentially ‘good’ ansatzes is named the candidate tree. Each node  $\mathbf{v}$  in the tree maintains a leaf count  $c_l(\mathbf{v})$  to indicate the number of leaf nodes below  $\mathbf{v}$  and a training count  $c_t(\mathbf{v})$  to record the total times of training of the node. At each path sampling procedure, the GSA samples a path from the candidate tree with the probability  $\epsilon_1$  and from the  $\mathbb{S}(N_l)$  uniformly with the probability  $1 - \epsilon_1$ . While sampling from the candidate tree, nodes are successively sampled from the root to a leaf. Since only potentially ‘good’ ansatzes are appended on the candidate tree and recorded the training count of nodes via the one-shot training scheme, nodes in the candidate tree with large training count may intuitively have more probability to construct potentially ‘good’ ansatzes. Let the last selected node be  $\mathbf{v}^{l-1}$ ,

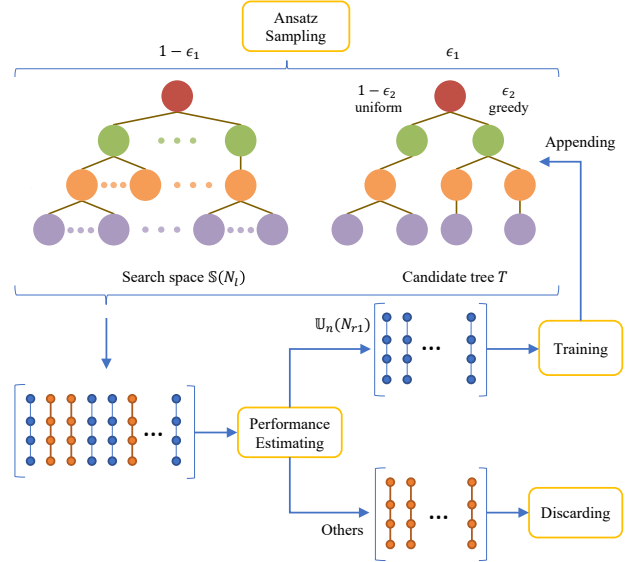


Figure 2: Single iteration of *pool training* with  $N_l = 3$ .

$1 \leq l \leq N_l$ , linked to child nodes  $\mathbf{v}_1^l, \mathbf{v}_2^l, \dots, \mathbf{v}_{N_v}^l$ . Then, the next node is sampled as  $\mathbf{v}_k^l$  with the probability

$$\Pr(\mathbf{v}_k^l; \eta) = \frac{c_l(\mathbf{v}_k^l) + \eta c_t(\mathbf{v}_k^l)}{\sum_{i=1}^{N_v} c_l(\mathbf{v}_i^l) + \eta c_t(\mathbf{v}_i^l)}, \quad (32)$$

where  $\eta = 1$  with the probability  $\epsilon_2$  representing the greedy sampling and  $\eta = 0$  with the probability  $1 - \epsilon_2$  representing the uniform sampling. The ansatz sampling procedure is summarized as Alg.3.

As depicted in Fig. 2, at each main process iteration of the *pool training*, the GSA samples  $N_{s1}$  paths exploiting the double  $\epsilon$ -greedy strategy. Then, the cost function values and gradients of sampled ansatzes are estimated with corresponding parameters from the parameter pool. Subsequently, the  $N_{r1}$ -rank solution  $\mathbb{U}_n(N_{r1})$  of Prob.3 are determined among the sampled ansatzes. For each ansatz  $U \in \mathbb{U}_n(N_{r1})$ , corresponding parameters in parameter pool are updated in single step via gradient decent optimizer. The main process terminates at iteration  $N_{t1}$  or when  $c_l(\mathbf{v}^0)$  is stable that the value has been preserved for  $N_{t1}$  iterations which means there is no new paths appended on the tree. As a result, the main process of the *pool training* is summarized as Alg.4.

For the stability of *pool training*, we provide a prethermalization before the main process iterations. Given the  $N_{i0}$ , at iteration  $i$ , the GSA processes as a main process iteration with the  $\epsilon'_1 = (i - 1)\epsilon_1/N_{i0}$  instead of  $\epsilon_1$ , respectively.

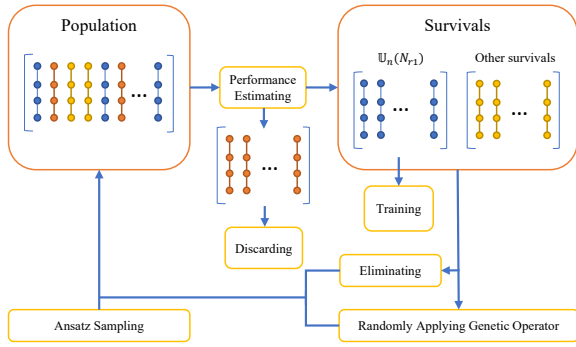


Figure 3: Single generation of *alternate training*.

The prethermalization of *pool training* is summarized as Alg.5.

Finally, the *pool training* can be described by Alg.6. After the initialization of  $P$  and  $T$ , the prethermalization and the main process are conducted to train  $P$  as well as  $T$ . Subsequently, the set of parameters  $\mathbb{P}_0$  can be constructed by expand  $P$  that for each ansatz  $U$  in  $\mathbb{S}(N_I)$ ,  $\theta_U$  is generated by Eq.(30). The  $\mathbb{P}_0$  and  $T$  are output for the next stage.

### 4.3 Alternate training

Recall that the VA-VQE can be solved via alternately solving Prob.3 and Prob.1. We exploit the multi-objective genetic algorithm with novel modification. The set of parameters  $\mathbb{P}$  are initialized as  $\mathbb{P}_0$ . The individuals in the first generation are sampled independently via double  $\epsilon$ -greedy strategy as described in Sec.4.2 to compose the initial population.

As shown in Fig.3, at each generation (iteration), ansatzes in the  $\mathbb{U}_n(N_{r2})$  of Prob.3 with respect to the population are trained to update  $\mathbb{P}$  in  $N_o$  steps via gradient decent optimizer. Note that the number of ansatzes in  $\mathbb{U}_n(N_{r2})$  should be less than  $N_{s2}/2$ . Similar to traditional genetic algorithm NGSA-II,  $N_{s2}/2$  ansatzes are survived. Specifically, the GSA finds a  $N'_r$  such that

$$|\mathbb{U}_n(N'_r)| < N_{s2}/2 \leq |\mathbb{U}_n(N'_r + 1)|.$$

Then, ansatzes are sequentially add to survivals in increasing order of cost function value from  $\mathbb{U}_n(N'_r + 1) \setminus \mathbb{U}_n(N'_r)$ . Subsequently, new ansatzes are generated via applying asexual genetic operators on survivals to fill the population. We leave the description of asexual genetic operators in Appendix.D. Besides, we introduce the explicit

elimination to the near-completely trained survivals  $U$  satisfying  $\alpha \frac{\|\nabla C(U, \theta_U)\|_2}{|\theta_U|} < \xi$ , where  $\alpha$  is the step size. The eliminated ansatz is record if it has the temporarily lowest cost function value and is erased if there exist an ansatz with lower cost function value. Notice that the elimination is conducted after the applying of genetic operators. Therefore, double  $\epsilon$ -greedy based sampling is required to refill the population.

The *alternate training* terminates at the generation  $N_{i2}$  or when the record eliminated ansatz is preserved for  $N_{t2}$  generations. As a result, the ansatz  $U^*$  with temporarily lowest cost function value is output as the quasi-optimal ansatz. Meanwhile, the corresponding parameters  $\theta_{U^*}$  is output for the next stage as the parameter initialization. We summarize the *alternate training* in Alg.7.

### 4.4 VQE retraining

The final stage *VQE retraining* inherits the quasi-optimal ansatz  $\theta_{U^*}$  and corresponding parameters  $\theta_{U^*}$  output from the *alternate training*, and provide a guarantee to sufficiency of the parameter training of  $\theta_{U^*}$ . As traditional VQE training does, this stage simply trains the parameters of  $\theta_{U^*}$  with the initialization  $\theta_{U^*}$  until the cost function value converges or the iteration count reaches  $N_{i3}$ . We summarize this stage as Alg.8 for completeness.

## 5 Numerical Simulations

To showcase the improvement of the proposed framework, we compare it with structure fixed hardware efficient ansatz (HEA) [16], the QAS [17] and a fully randomized (RND) baseline algorithm. To make a fair comparison, we use Python with *PennyLane* package [46] to implement both our and the three compared algorithms. The technique details for algorithms to be compared are elaborated as follows:

- **HEA.** HEA utilizes a fixed layer pattern to construct the whole circuit. The layer construction used in this implementation is depicted in Appendix B. Note that this kind of ansatzes is also widely used in other implementations, e.g., [10, 11];

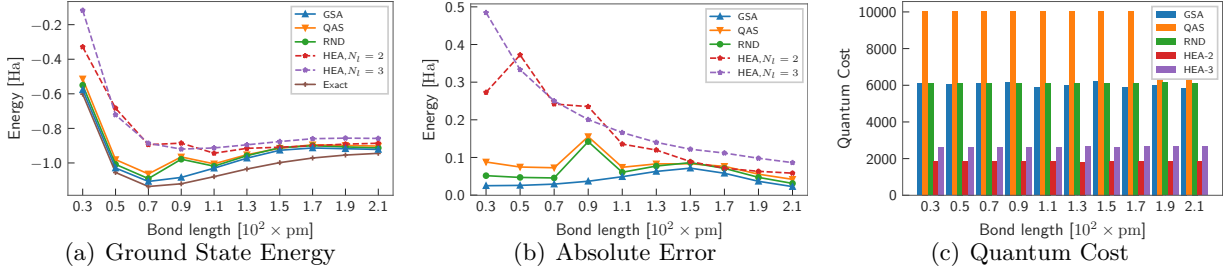


Figure 4: The average result of determining ground state energy of  $H_2$  with various bond lengths among 100 running times.

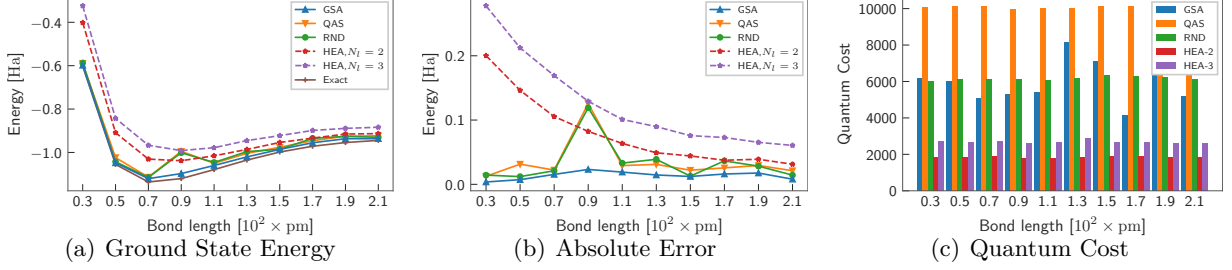


Figure 5: The best result of determining ground state energy of  $H_2$  with various bond lengths among 100 running times.

- **QAS.** QAS utilizes weight sharing strategy and adversarial bandit training technique to implement the VA-VQE. Its outstanding performance has been experimentally proved in [47];
- **RND.** We sample  $N_{Rs}$  circuits with unique random parameters, then process the VQE retraining and output the circuit with the minimum cost function value.

We assume that the depolarization dominate the quantum error in the quantum hardware. Then, the noise operator (depolarizing channel) is

$$\Phi(p, \sigma) = \sum_{i=0}^3 K_i(p) \sigma K_i^\dagger(p),$$

$$K_0 = \sqrt{1-p} \begin{bmatrix} 1 & 0 \\ 0 & 1 \end{bmatrix}, K_1 = \sqrt{\frac{p}{3}} \begin{bmatrix} 0 & 1 \\ 1 & 0 \end{bmatrix},$$

$$K_2 = \sqrt{\frac{p}{3}} \begin{bmatrix} 0 & -i \\ i & 0 \end{bmatrix}, K_3 = \sqrt{\frac{p}{3}} \begin{bmatrix} 1 & 0 \\ 0 & -1 \end{bmatrix},$$

where  $p \in [0, 1]$  is the depolarization probability,  $\sigma$  is a density matrix of single qubit [46]. In our configuration, a depolarizing channel with depolarization probability  $p = 0.001$  is applied after a single qubit gate. We simultaneously apply two

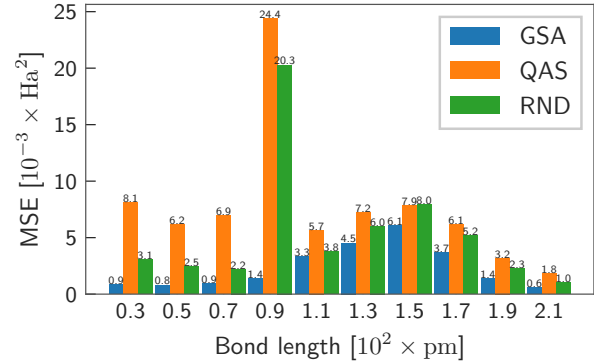


Figure 6: Mean square error among 100 running times.

depolarizing channels with depolarization probability  $p = 0.01$  after a CNOT, i.e., apply one on the control qubit, and one on the target qubit.

The criteria used for all methods are absolute error between the obtained and exact optimal cost function values, the invoking times for the calculation of the cost function (termed *quantum cost* henceforth), respectively. For VA-VQE, we analyze the distribution of performances of output ansatzes and calculate the mean square error (MSE) mathematically represented by

$$MSE = \frac{1}{M} \sum_{i=1}^M (\hat{C}_i^* - C_{exact}^*)^2 \quad (33)$$

to indicate the stability to obtain the quasi-

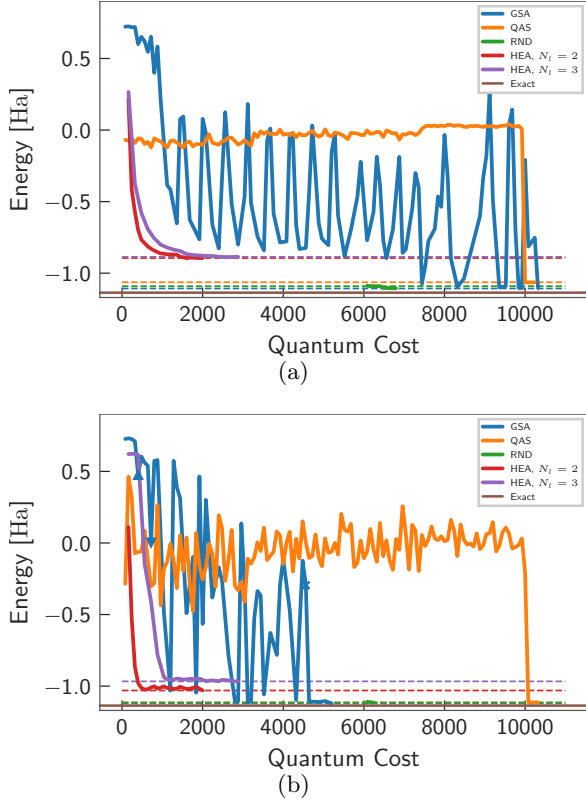


Figure 7: Detail of cost function values with respect to quantum cost in solving the ground state energy of  $H_2$  with bond length  $0.7 \times 10^2$  pm among 100 running times. (a) The average cost function values with respect to quantum cost. (b) The cost function values among 100 running times with respect to quantum cost in the running time which output the ansatz with the lowest cost function value among 100 running times. The  $\blacktriangle$ ,  $\blacktriangledown$  and  $\times$  represent the termination of *pool training*'s prethermalization, *pool training*'s main process and *alternate training*, respectively.

optimal cost function values, where  $M$  is the total running time,  $\hat{C}^*$  is the output quasi-optimal cost function value and  $C_{exact}^*$  is the exact optimal cost function value.

We conduct numerical simulations on determining the ground state energies of Hamiltonians of  $H_2$  [48] with various bond lengths. The quantum device is assumed to have 4 qubits with ring connectives and depolarization error being imposed by the classical simulator. For the proposed framework, we empirical set  $N_l = 3$ ,  $\alpha_0 = 5$ ,  $\xi = 0.003$ ,  $\epsilon_1 = \epsilon_2 = 0.8$ ,  $N_{s1} = N_{s2} = 16$ ,  $N_{r1} = 1$ ,  $N_{r2} = 2$ ,  $N_{i0} = N_{i1} = 2$ ,  $N_{i2} = 100$ ,  $N_{i3} = 10$ ,  $N_{t1} = 1$ ,  $N_{t2} = 4$ ,  $N_o = 5$ ; for HEA, the we exploit 2-layer HEA as HEA-2 and 3-layer HEA as HEA-3; for QAS, we follows the default configurations, where  $N_l = 3$ , the number of su-

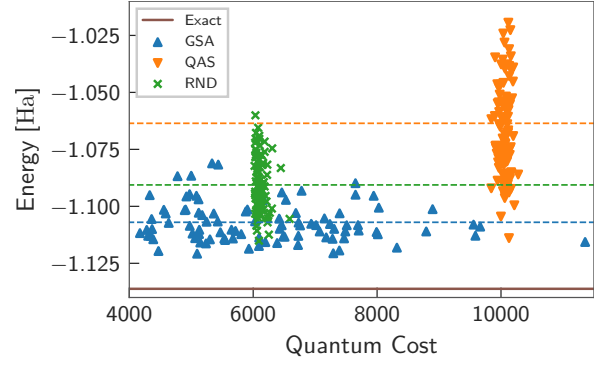


Figure 8: Output quasi-optimal cost function values with respect to quantum cost of 100 running times in solving the ground state energy of  $H_2$  with bond length  $0.7 \times 10^2$  pm. Dashed lines present cost function values in average.

pernets  $N_W = 5$ , the number of iterations in supernet training  $N_T = 400$  (include 200 warm up iterations), the number of sampled subnets for ranking  $N_K = 500$ ; for RND, we set  $N_l = 3$  and  $N_{Rs} = 6000$  such that the quantum costs of GSA and RND are approximately equal.

For each bond length, we conduct the GSA and comparison methods 100 times, respectively. The results in average are shown in Fig. 4. It can be found that our algorithm can determine ground state energy with consistently lower absolute error in average than the compared algorithms in terms of the absolute error under various bond lengths, and with lower quantum cost compared to QAS and RND. This conclusion holds while considering the ansatzes with lowest cost function values among the 100 running times as depicted in Fig. 5. Moreover, GSA exhibit out standing stability as shown in Fig. 6. It is clear that VA-VQE methods performs better in terms of absolute error at a cost of quantum cost than HEA with most bond lengths. However, the elaborate VA-VQE methods may not generate an ansatz with lower cost function value and higher stability than the full-randomized RND method in small-scale tasks.

For bond length  $0.7 \times 10^2$  pm, we also record the quantum cost and absolute error for each running time in Fig. 7 and Fig. 8 when the algorithm converges to the final output result. It can be concluded that our algorithm is able to obtain the best solution in average with a rather small quantum cost (about 6107.49) which is conspicuously better than HEA (up to 87.9% improvement in terms of error), QAS (up to 59.8%, 39.3%

and 86.8% improvement in terms of error, quantum cost and stability, respectively) and RND (up to 36.0% and 58.7% improvement in terms of error and stability, respectively). Remarkably, GSA can asymptotically reach the best ansatz among the training, which means that a temporarily quasi-optimal ansatz can be output at any generation of *alternate training*. Termination conditions of the three stages are reasons for the large variance of quantum cost of GSA.

## 6 Conclusion

In this paper, addressing the issues in mitigating BP phenomenon in VQE, we propose a gradient sensitive alternate framework for VQE with variable ansatz strategy. We propose a theoretical framework which highlight the magnitude of gradient and exploit the alternate optimization scheme, so that the local optimum can be avoid from the ansatz perspective. It can be theoretically proved that the result of proposed theoretical framework is a subset of results of original VA-VQE.

Then, based on the theoretical framework, an novel implementation GSA is proposed with three stages. We reduce the size of search space of the ansatz via applying gate commutation rules and establishing a bijection between the search space and the practical implementations of ansatzes to boost the time efficiency of the optimal ansatz and parameter determination. Exploiting the candidate tree based double  $\epsilon$ -greedy strategy, an initialization of parameters are determined, so that the training competitions are mitigated and the local optimal can be evaded from the parameter perspective. Based on the initialization of parameters, the GSA follows the framework with modified genetic algorithm to find and train a quasi-optimal ansatz.

Finally, we conduct the numerical simulations on quantum chemistry to find the ground state energy of a quantum system. We adopt relatively fair criteria for measuring the performance of VA-VQE, so that the transverse comparison among methods of VA-VQE can be clearly conducted. As a result, the GSA shows conspicuously better performance in average compared to the structure fixed HEA up to 87.9% improvement in terms of absolute error, to the QAS up to 59.8%, 39.3% and 86.8% improvement in terms of absolute er-

ror, quantum cost and stability, respectively, and to the full-randomized RND up to 36.0% and 58.7% improvement in terms of error and stability respectively.

Although the proposed method obtained better results, there are more researches required to be conducted. For example, GSA requires a number of hyperparameters to be adjusted such as  $N_l$ . Automatic hyperparameter adjustment may be a meaningful research on the VA-VQE.

## Acknowledgements

This work was supported by the National Science Foundation of China (No. 61871111 and No. 61960206005) and the Fundamental Research Funds for the Central Universities (No. 2242022k30006 and No. 2242022k30001).

## References

- [1] Lov K Grover. “Quantum computers can search arbitrarily large databases by a single query”. *Physical review letters* **79**, 4709 (1997).
- [2] Peter W Shor. “Polynomial-time algorithms for prime factorization and discrete logarithms on a quantum computer”. In *SIAM Review*. Volume 41, pages 303–332. SIAM (1999).
- [3] Aram W. Harrow, Avinatan Hassidim, and Seth Lloyd. “Quantum algorithm for linear systems of equations”. *Physical review letters* **103**, 150502 (2009).
- [4] Guang Hao Low and Isaac L. Chuang. “Hamiltonian simulation by qubitization”. *Quantum* **3**, 163 (2019).
- [5] John Preskill. “Quantum computing in the NISQ era and beyond”. *Quantum* **2**, 79 (2018).
- [6] Alberto Peruzzo, Jarrod McClean, Peter Shadbolt, Man-Hong Yung, Xiao-Qi Zhou, Peter J. Love, Alán Aspuru-Guzik, and Jeremy L. O’Brien. “A variational eigenvalue solver on a photonic quantum processor”. *Nature communications* **5**, 1–7 (2014).
- [7] Carlos Bravo-Prieto, Ryan LaRose, M. Cerezo, Yigit Subasi, Lukasz Cincio, and Patrick J. Coles. “Variational Quantum Linear Solver” (2020). [arXiv:1909.05820](https://arxiv.org/abs/1909.05820).



- [8] Xiao Yuan, Suguru Endo, Qi Zhao, Ying Li, and Simon C. Benjamin. “Theory of variational quantum simulation”. *Quantum* **3**, 191 (2019).
- [9] Xin Wang, Zhixin Song, and Youle Wang. “Variational quantum singular value decomposition”. *Quantum* **5**, 483 (2021).
- [10] Fan-Xu Meng, Ze-Tong Li, Xutao Yu, and Zaichen Zhang. “Quantum algorithm for MUSIC-based DOA estimation in hybrid MIMO systems”. *Quantum Science and Technology* (2021).
- [11] Ze-Tong Li, Fan-Xu Meng, Xu-Tao Yu, and Zai-Chen Zhang. “Quantum algorithm for Laplacian eigenmap via Rayleigh quotient iteration”. *Quantum Information Processing* **21**, 1–20 (2022).
- [12] Kerstin Beer, Dmytro Bondarenko, Terry Farrelly, Tobias J. Osborne, Robert Salzmann, Daniel Scheiermann, and Ramona Wolf. “Training deep quantum neural networks”. *Nature Communications* **11**, 808 (2020).
- [13] Amira Abbas, David Sutter, Christa Zoufal, Aurelien Lucchi, Alessio Figalli, and Stefan Woerner. “The power of quantum neural networks”. *Nature Computational Science* **1**, 403–409 (2021).
- [14] Jacob Biamonte, Peter Wittek, Nicola Pancotti, Patrick Rebentrost, Nathan Wiebe, and Seth Lloyd. “Quantum machine learning”. *Nature* **549**, 195–202 (2017).
- [15] Vojtěch Havlíček, Antonio D. Córcoles, Kristan Temme, Aram W. Harrow, Abhinav Kandala, Jerry M. Chow, and Jay M. Gambetta. “Supervised learning with quantum-enhanced feature spaces”. *Nature* **567**, 209–212 (2019).
- [16] Abhinav Kandala, Antonio Mezzacapo, Kristan Temme, Maika Takita, Markus Brink, Jerry M Chow, and Jay M Gambetta. “Hardware-efficient variational quantum eigensolver for small molecules and quantum magnets”. *Nature* **549**, 242–246 (2017).
- [17] Yuxuan Du, Tao Huang, Shan You, Min-Hsiu Hsieh, and Dacheng Tao. “Quantum circuit architecture search: Error mitigation and trainability enhancement for variational quantum solvers” (2020). [arXiv:2010.10217](https://arxiv.org/abs/2010.10217).
- [18] Jarrod R McClean, Sergio Boixo, Vadim N Smelyanskiy, Ryan Babbush, and Hartmut Neven. “Barren plateaus in quantum neural network training landscapes”. *Nature communications* **9**, 1–6 (2018).
- [19] Taylor L. Patti, Khadijeh Najafi, Xun Gao, and Susanne F. Yelin. “Entanglement devised barren plateau mitigation”. *Physical Review Research* **3**, 033090 (2021).
- [20] Carlos Ortiz Marrero, Mária Kieferová, and Nathan Wiebe. “Entanglement-Induced Barren Plateaus”. *PRX Quantum* **2**, 040316 (2021).
- [21] Marco Cerezo, Akira Sone, Tyler Volkoff, Lukasz Cincio, and Patrick J. Coles. “Cost function dependent barren plateaus in shallow parametrized quantum circuits”. *Nature communications* **12**, 1–12 (2021).
- [22] Stefan H. Sack, Raimel A. Medina, Alexios A. Michailidis, Richard Kueng, and Maksym Serbyn. “Avoiding barren plateaus using classical shadows” (2022). [arXiv:2201.08194](https://arxiv.org/abs/2201.08194).
- [23] Zoë Holmes, Kunal Sharma, M. Cerezo, and Patrick J. Coles. “Connecting ansatz expressibility to gradient magnitudes and barren plateaus”. *PRX Quantum* **3**, 010313 (2022). [arXiv:2101.02138](https://arxiv.org/abs/2101.02138).
- [24] Samson Wang, Enrico Fontana, Marco Cerezo, Kunal Sharma, Akira Sone, Lukasz Cincio, and Patrick J. Coles. “Noise-induced barren plateaus in variational quantum algorithms”. *Nature communications* **12**, 1–11 (2021).
- [25] Arthur G. Rattew, Shaohan Hu, Marco Pistoia, Richard Chen, and Steve Wood. “A Domain-agnostic, Noise-resistant, Hardware-efficient Evolutionary Variational Quantum Eigensolver” (2020). [arXiv:1910.09694](https://arxiv.org/abs/1910.09694).
- [26] Shi-Xin Zhang, Chang-Yu Hsieh, Shengyu Zhang, and Hong Yao. “Differentiable Quantum Architecture Search” (2021). [arXiv:2010.08561](https://arxiv.org/abs/2010.08561).
- [27] Mateusz Ostaszewski, Lea M. Trenkwalder, Wojciech Masarczyk, Eleanor Scerri, and Vedran Dunjko. “Reinforcement learning for optimization of variational quantum circuit architectures”. In *Advances in Neural Information Processing Systems*. **Volume 34**, pages 18182–18194. Curran Associates, Inc. (2021).

- [28] M. Bilkis, M. Cerezo, Guillaume Verdon, Patrick J. Coles, and Lukasz Cincio. “A semi-agnostic ansatz with variable structure for quantum machine learning” (2022). [arXiv:2103.06712](#).
- [29] Zi-Jian Zhang, Thi Ha Kyaw, Jakob Kottmann, Matthias Degroote, and Alan Aspuru-Guzik. “Mutual information-assisted adaptive variational quantum eigensolver”. *Quantum Science and Technology* (2021).
- [30] Fanxu Meng, Ze-Tong Li, Xu-Tao Yu, and Zai-Chen Zhang. “Quantum Circuit Architecture Optimization for Variational Quantum Eigensolver via Monto-Carlo Tree Search”. *IEEE Transactions on Quantum Engineering* (2021).
- [31] D. Chivilikhin, A. Samarin, V. Ulyantsev, I. Iorsh, A. R. Oganov, and O. Kyriienko. “MoG-VQE: Multiobjective genetic variational quantum eigensolver” (2020). [arXiv:2007.04424](#).
- [32] Thomas Elsken, Jan Hendrik Metzen, and Frank Hutter. “Neural Architecture Search: A Survey” (2019). [arXiv:1808.05377](#).
- [33] Kosuke Mitarai, Makoto Negoro, Masahiro Kitagawa, and Keisuke Fujii. “Quantum circuit learning”. *Physical Review A* **98**, 032309 (2018).
- [34] Philip Wolfe. “Convergence conditions for ascent methods”. *SIAM review* **11**, 226–235 (1969).
- [35] Sukin Sim, Peter D. Johnson, and Alán Aspuru-Guzik. “Expressibility and entangling capability of parameterized quantum circuits for hybrid quantum-classical algorithms”. *Advanced Quantum Technologies* **2**, 1900070 (2019).
- [36] Kouhei Nakaji and Naoki Yamamoto. “Expressibility of the alternating layered ansatz for quantum computation”. *Quantum* **5**, 434 (2021).
- [37] Marco Cerezo and Patrick J. Coles. “Higher order derivatives of quantum neural networks with barren plateaus”. *Quantum Science and Technology* **6**, 035006 (2021).
- [38] Andrew Arrasmith, M. Cerezo, Piotr Czarnik, Lukasz Cincio, and Patrick J. Coles. “Effect of barren plateaus on gradient-free optimization”. *Quantum* **5**, 558 (2021).
- [39] Daniel Stilck França and Raul Garcia-Patron. “Limitations of optimization algorithms on noisy quantum devices”. *Nature Physics* **17**, 1221–1227 (2021).
- [40] Arthur Pesah, M. Cerezo, Samson Wang, Tyler Volkoff, Andrew T. Sornborger, and Patrick J. Coles. “Absence of barren plateaus in quantum convolutional neural networks”. *Physical Review X* **11**, 041011 (2021).
- [41] Tyler Volkoff and Patrick J. Coles. “Large gradients via correlation in random parameterized quantum circuits”. *Quantum Science and Technology* **6**, 025008 (2021).
- [42] Andrea Skolik, Jarrod R. McClean, Masoud Mohseni, Patrick van der Smagt, and Martin Leib. “Layerwise learning for quantum neural networks”. *Quantum Machine Intelligence* **3**, 1–11 (2021).
- [43] Edward Grant, Leonard Wossnig, Mateusz Ostaszewski, and Marcello Benedetti. “An initialization strategy for addressing barren plateaus in parametrized quantum circuits”. *Quantum* **3**, 214 (2019).
- [44] Guillaume Verdon, Michael Broughton, Jarrod R. McClean, Kevin J. Sung, Ryan Babush, Zhang Jiang, Hartmut Neven, and Masoud Mohseni. “Learning to learn with quantum neural networks via classical neural networks” (2019). [arXiv:1907.05415](#).
- [45] Shan You, Tao Huang, Mingmin Yang, Fei Wang, Chen Qian, and Changshui Zhang. “GreedyNAS: Towards fast one-shot NAS with greedy supernet”. In Proceedings of the IEEE/CVF Conference on Computer Vision and Pattern Recognition. *Pages 1999–2008*. IEEE (2020).
- [46] Ville Bergholm, Josh Izaac, Maria Schuld, Christian Gogolin, M. Sohaib Alam, Shahnawaz Ahmed, Juan Miguel Arrazola, Carsten Blank, Alain Delgado, Soran Jahangiri, Keri McKiernan, Johannes Jakob Meyer, Zeyue Niu, Antal Száva, and Nathan Killoran. “PennyLane: Automatic differentiation of hybrid quantum-classical computations” (2020). [arXiv:1811.04968](#).
- [47] Kehuan Linghu, Yang Qian, Ruixia Wang, Meng-Jun Hu, Zhiyuan Li, Xuegang Li, Huikai Xu, Jingning Zhang, Teng Ma, Peng Zhao, Dong E. Liu, Min-Hsiu Hsieh, Xingyao Wu, Yuxuan Du, Dacheng Tao, Yirong Jin, and Haifeng Yu. “Quantum circuit architecture search on a superconducting processor” (2022). [arXiv:2201.00934](#).

- [48] Nikolay V. Tkachenko, James Sud, Yu Zhang, Sergei Tretiak, Petr M. Anisimov, Andrew T. Arrasmith, Patrick J. Coles, Lukasz Cincio, and Pavel A. Dub. “Correlation-informed permutation of qubits for reducing ansatz depth in the variational quantum eigensolver”. *PRX Quantum* **2**, 020337 (2021).

## A Examples

**Example 1** (A VQE Task). *The VQE is to find the ground state energy of a quantum system where the dynamic can be described by a Hamiltonian  $H$ . Setting the observable  $O = H$ , the function  $f(x) = x$ , the input state  $\rho = |0\rangle\langle 0|$  and the ansatz  $U(\boldsymbol{\theta})$  as the hardware efficient ansatz (c.f. Appendix B), where  $\boldsymbol{\theta} \in (-\pi, \pi]^d$  and  $d$  is the number of parameters, the problem is*

$$\min_{\boldsymbol{\theta} \in (-\pi, \pi]^d} C(\boldsymbol{\theta}) = \text{Tr} \left[ H U(\boldsymbol{\theta}) |0\rangle\langle 0| U^\dagger(\boldsymbol{\theta}) \right]. \quad (34)$$

**Example 2** (Not Bijection). *For a 2-qubit quantum system,  $N_l = 2$ , define  $\mathbf{s}_1$  and  $\mathbf{s}_2$  as  $(I^{q_1}, R_y^{q_2})$  and  $(R_y^{q_1}, I^{q_2})$ , respectively. Then, the practical implementations of two ansatzes described by paths*

$$\begin{aligned} \mathbf{p}_1 &= (\mathbf{v}^0, \mathbf{v}_1^1 := (\mathbf{v}^0, \mathbf{s}_1), \mathbf{v}_1^2 := (\mathbf{v}^1, \mathbf{s}_2)), \\ \mathbf{p}_2 &= (\mathbf{v}^0, \mathbf{v}_2^1 := (\mathbf{v}^0, \mathbf{s}_2), \mathbf{v}_2^2 := (\mathbf{v}^1, \mathbf{s}_1)) \end{aligned}$$

*are identical.*

**Example 3** (Mergeable & Deletable). *For a 4-qubit quantum system,  $N_l = 2$ , define*

$$\begin{aligned} \mathbf{s}_1 &:= (I^{q_1}, R_y^{q_2}, CNOT^{q_3, q_4}), \\ \mathbf{s}_2 &:= (R_z^{q_1}, R_y^{q_2}, CNOT^{q_3, q_4}), \\ \mathbf{s}_3 &:= (R_z^{q_1}, R_y^{q_2}). \end{aligned}$$

*Then, the practical implementations of two ansatzes described by paths*

$$\begin{aligned} \mathbf{p}_1 &= (\mathbf{v}^0, \mathbf{v}_1^1 := (\mathbf{v}^0, \mathbf{s}_1), \mathbf{v}_1^2 := (\mathbf{v}^1, \mathbf{s}_2)), \\ \mathbf{p}_2 &= (\mathbf{v}^0, \mathbf{v}_2^1 := (\mathbf{v}^0, \mathbf{s}_3), \mathbf{v}_2^2 := (\mathbf{v}^1, ( ))) \end{aligned}$$

*are equivalent.*

**Example 4** (Size of Search Space). *The number of possible paths in a 4-qubit quantum system under the setting as described in Sec. 2.6 with and without the gates commutation rules  $N_{w/}$  and  $N_{w/o}$  with respect to  $N_l$  are demonstrated in Tab.1*

Table 1: The number of possible paths with respect to  $N_l$ .

$N_l$	$N_{w/}$	$N_{w/o}$	$\frac{N_{w/}}{N_{w/o}}$
1	56	567	9.88%
2	11768	321489	3.66%
3	2859977	182284263	1.57%

## B Hardware efficient ansatz

The hardware efficient ansatz (HEA) was first proposed in [16] to conduct VQE for small molecules and quantum magnets. It is constructed in a layer-by-layer fashion in which each layer has identical structure. Specifically, a layer is organized by native single qubit gates on all qubits and naturally available entangling interactions. In our setting, based on the native gates as described in Sec.2.6, we exploit the HEA with layers as depicted in Fig.9.

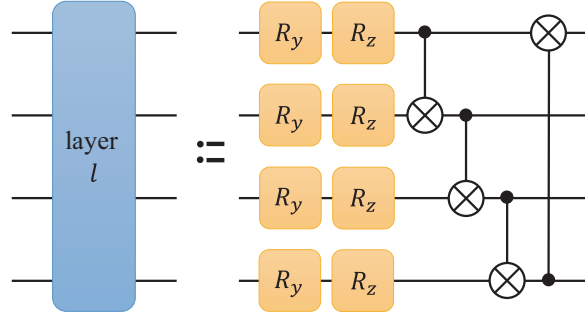


Figure 9: Layer construction used in HEA.

## C Proof of Theorem 1

Solutions of Prob.1 is a set of parameters

$$\Theta^* = \{\theta^* | C(\theta^*) = \min_{\theta \in \mathbb{D}^d} C(\theta)\}. \quad (35)$$

$$\left\{ (U^*, \Theta^*) \left| \begin{array}{l} C(U^*, \theta^*) = \min_{U, \theta} C(U, \theta), \\ \forall \theta^* \in \Theta^* \end{array} \right. \right\}. \quad (36)$$

Given an arbitrary valid  $\mathbb{P}$ , we divide  $\mathbb{G}^\infty$  into four disjoint sets

$$\mathbb{U}_+^* \equiv \left\{ U \left| C(U, \theta_U) = \min_{U, \theta} C(U, \theta) \right. \right\}, \quad (37)$$

$$\mathbb{U}_+ \equiv \left\{ U \left| \exists \theta', C(U, \theta') = \min_{U, \theta} C(U, \theta), C(U, \theta_U) > \min_{\theta} C(U, \theta) \right. \right\}, \quad (38)$$

$$\mathbb{U}_-^* \equiv \left\{ U \left| \forall \theta', C(U, \theta') > \min_{U, \theta} C(U, \theta), C(U, \theta_U) = \min_{\theta} C(U, \theta) \right. \right\}, \quad (39)$$

$$\mathbb{U}_- \equiv \left\{ U \left| \forall \theta', C(U, \theta') > \min_{U, \theta} C(U, \theta), C(U, \theta_U) > \min_{\theta} C(U, \theta) \right. \right\}. \quad (40)$$

Note that  $\mathbb{U}_+^* \cup \mathbb{U}_+ \cup \mathbb{U}_-^* \cup \mathbb{U}_- = \mathbb{G}^\infty$ . We prove the theorem by proving

$$\lim_{t \rightarrow \infty} \mathbb{U}_n \cap (\mathbb{U}_-^* \cup \mathbb{U}_-) = \emptyset, \quad (41)$$

$$\lim_{t \rightarrow \infty} \mathbb{U}_n = \lim_{t \rightarrow \infty} \mathbb{U}_+^*, \quad (42)$$

where  $t$  is the iterations of the alternate optimization loop.

**Lemma 1.**  $U \in \lim_{t \rightarrow \infty} \mathbb{U}_+^* \cup \mathbb{U}_-^*, \forall U \in \mathbb{U}_+ \cup \mathbb{U}_-$  such that  $\frac{\|\nabla C(U, \theta_U)\|_2}{|\theta_U|} > 0$ .

*Proof.* By solving the Prob.3,  $\forall U \in \mathbb{U}_+ \cup \mathbb{U}_-$  such that  $\frac{\|\nabla C(U, \theta_U)\|_2}{|\theta_U|} = \max_{\theta} \frac{\|\nabla C(U, \theta)\|_2}{|\theta|} > 0$  are included in  $\mathbb{U}_n$ . For all  $U \in \mathbb{U}_n$ , the  $\theta_U \in \mathbb{P}$  are updated by  $\theta^*$  such that  $C(U, \theta^*) = \min_{\theta} C(U, \theta)$ , which means  $\forall U \in \mathbb{U}_n$  are elements of  $U \in \mathbb{U}_+^* \cup \mathbb{U}_-^*$  in the next iteration. Therefore, all  $U \in \mathbb{U}_+ \cup \mathbb{U}_-$  such that  $\frac{\|\nabla C(U, \theta_U)\|_2}{|\theta_U|} > 0$  will be selected as an element in  $\mathbb{U}_n$  if  $t \rightarrow \infty$ . Then, we have  $U \in \lim_{t \rightarrow \infty} \mathbb{U}_+^* \cup \mathbb{U}_-^*$ ,  $\forall U \in \mathbb{U}_+ \cup \mathbb{U}_-$  such that  $\frac{\|\nabla C(U, \theta_U)\|_2}{|\theta_U|} > 0$ .  $\square$

Further, it is straightforward that  $U \in \lim_{t \rightarrow \infty} \mathbb{U}_+^*, \forall U \in \mathbb{U}_+$  such that  $\frac{\|\nabla C(U, \theta_U)\|_2}{|\theta_U|} > 0$  and  $V \in \lim_{t \rightarrow \infty} \mathbb{U}_-^*, \forall V \in \mathbb{U}_-$  such that  $\frac{\|\nabla C(V, \theta_V)\|_2}{|\theta_V|} > 0$ . Since  $C(U, \theta_U) = \min_{\theta} C(U, \theta)$  for all  $U \in \mathbb{U}_+^* \cup \mathbb{U}_-^*$ , we have that

$$\frac{\|\nabla C(U, \theta_U)\|_2}{|\theta_U|} = 0, \forall U \in \mathbb{U}_+^* \cup \mathbb{U}_-^*. \quad (43)$$



Therefore, if  $\mathbb{U}_+^*$  is not empty, inequalities Eq.25 and Eq.26 are simultaneously established for all  $U \in \mathbb{U}_-^*$ ,  $V \in \mathbb{U}_+^*$ , which means  $\mathbb{U}_n \cap \mathbb{U}_-^* = \emptyset$ . Then, we have that

$$\lim_{t \rightarrow \infty} \mathbb{U}_n \cap (\mathbb{U}_-^* \cup \mathbb{U}_-) = \emptyset, \quad (44)$$

if  $\lim_{t \rightarrow \infty} \mathbb{U}_+^* \neq \emptyset$ .

The establishment of Eq.(27) and Eq.(28) of  $V$  implies that  $V \in \mathbb{U}_+$  with  $\frac{\|\nabla C(V, \theta_V)\|_2}{|\theta_V|} > 0$  or  $V \in \mathbb{U}_+^*$ , which indicates

$$\lim_{t \rightarrow \infty} \mathbb{U}_+^* \neq \emptyset. \quad (45)$$

It is obvious that  $\mathbb{U}_+^* \subset \mathbb{U}_n$  and  $\mathbb{U}_n \subset \mathbb{U}_+^* \cup \mathbb{U}_+$ . Since

$$\lim_{t \rightarrow \infty} \mathbb{U}_+ \equiv \left\{ U \left| \begin{array}{l} \exists \theta', C(U, \theta') = \min_{U, \theta} C(U, \theta), \\ \forall \delta > 0, C(U, \theta_U) \in \lim_{t \rightarrow \infty} \mathbb{P} = \max_{\theta \in \Theta_{U, \delta}} C(U, \theta) \end{array} \right. \right\}, \quad (46)$$

where  $\Theta_{U, \delta} = \{\theta \mid \|\theta - \theta_U\|_2 < \delta\}$ , we have that  $\lim_{t \rightarrow \infty} (\mathbb{U}_n \cup \mathbb{U}_+) = \emptyset$ . Therefore, Eq.(41) and Eq.(42) are established.

## D Genetic Operators

In this appendix, we provide genetic operators the GSA applied in detail. We only consider the asexual genetic operators for the simplicity. Consequently, only single ansatz are generated from each survival ansatz. All genetic operators comply with the same structure. First, a new practical implementation of ansatz are randomly generated. Then, the implementation is refined by the gate commutation rule. Since the bijection between the search space and the practical implementations of ansatzes is established, the path representation of the new implementation is finally output. We introduce the genetic operators identified by the first step.

**Mutation:** The mutation operator randomly selects a node  $\mathbf{v}$  in the survival ansatz. Then, a child node  $\mathbf{v}_{new}$  of the parent node of  $\mathbf{v}$  is randomly sampled. Therefore, a new implementation of ansatz substituting  $\mathbf{v}$  by  $\mathbf{v}_{new}$  is generated.

**Deletion:** The deletion operator randomly deletes a node in the survival ansatz, and connects its parent node and child node. Then, a new implementation is generated.

**Amplification:** The amplification operator randomly select a node  $\mathbf{v}$  in the survival ansatz. Then, a child node of  $\mathbf{v}$  is inserted to the ansatz and therefore a new implementation is generated.

## E Pseudocodes for Algorithms

In this appendix, we list the pseudocodes for algorithms. Note that the task  $\mathbb{T}$  is generally omitted as the input parameters of algorithms without confusing.

---

**Algorithm 1:** alternate VA-VQE

---

```
Input:  $\mathbb{G}, \mathbb{P}_0$ 
begin
   $\mathbb{S} = \mathbb{G}^\infty$ ;
   $\mathbb{P} \leftarrow \mathbb{P}_0$ ;                                     // Initialize  $\mathbb{P}$ 
   $\mathbb{U}_n \leftarrow \{\}$ ;                                   // Initialize  $\mathbb{U}_n$ 
  while  $\mathbb{U}_n$  and  $\mathbb{P}$  are not converged do
     $\mathbb{U}_n \leftarrow \text{SolveProb3}(\mathbb{S}, \mathbb{P})$ ;
    foreach  $U \in \mathbb{U}_n$  do
       $\theta_U \in \mathbb{P} \leftarrow \text{SolveProb1}(U)$ ;
    end
  end
end
return  $\mathbb{U}_n, \mathbb{P}$ .
```

---

---

**Algorithm 2:** GSA

---

```
Input:  $\mathbb{G}$ 
begin
   $\mathbb{S}(N_l) \leftarrow$  Construct search space by  $\mathbb{G}$ ;
   $\mathbb{P}_0, T \leftarrow \text{PoolTraining}(\mathbb{S}(N_l))$ ;
   $U^*, \theta_{U^*} \leftarrow \text{AlternateTraining}(\mathbb{S}(N_l), \mathbb{P}_0, T)$ ;
   $U^*, \theta^* \leftarrow \text{VQETraining}(U^*, \theta_{U^*})$ ;
end
return  $U^*, \theta^*$ .
```

---

---

**Algorithm 3:** USampling

---

```
Input:  $\mathbb{S}(N_l), T, \epsilon_1, \epsilon_2$ 
begin
   $J_1 \sim \{(True, \epsilon_1), (False, 1 - \epsilon_1)\}$ ;
  if  $J_1$  is True then
     $\mathbf{v} \leftarrow \mathbf{v}^0 \in T$ ;
     $U \leftarrow (\mathbf{v})$ ;
     $\eta \sim \{(1, \epsilon_2), (0, 1 - \epsilon_2)\}$ ;
    for  $\mathbf{v}$  is not a leaf node do
       $\mathbb{V}_c \leftarrow \text{GetChildNodes}(\mathbf{v})$ ;
       $\mathbf{v}' \sim \{(\mathbf{v}'_k \in \mathbb{V}_c, \text{Pr}(\mathbf{v}'_k; \eta))\}$ ;
       $U \leftarrow U \oplus (\mathbf{v}')$ ;
       $\mathbf{v} \leftarrow \mathbf{v}'$ ;
    end
  else
     $U \sim \mathbb{S}(N_l)$ ;
  end
end
return  $U$ .
```

---

---

**Algorithm 4:** PoolTrainingMainProcess

---

**Input:**  $\mathbb{S}(N_l)$ ,  $P$ ,  $T$

```
begin
   $\mathbb{S} \leftarrow \mathbb{S}(N_l)$ ;
   $t \leftarrow 0$ ;
   $c'_l \leftarrow 1$ ;
   $i \leftarrow 1$ ;
  for  $i \leq N_{i1}$  do
     $\mathbb{U}_s \leftarrow \{\}$ ;
    for  $|\mathbb{U}_s| < N_{s1}$  do
       $U \leftarrow \text{USampling}(\mathbb{S}, T, \epsilon_1, \epsilon_2)$ ;
       $\mathbb{U}_s \leftarrow \mathbb{U}_s \cup \{U\}$ ;
    end
     $\mathbb{U}_n(N_{r1}) \leftarrow \text{SolveProb3}(\mathbb{U}_s, P)$ ;
    foreach  $U \in \mathbb{U}_n(N_{r1})$  do
       $\theta \leftarrow \text{GetParameters}(U, P)$ ;
       $\alpha \leftarrow \text{GetStepSize}(\alpha_0)$ ;
       $\theta \leftarrow \theta - \alpha \nabla C(U, \theta)$ ;
       $P \leftarrow \text{UpdatePool}(\theta, P)$ ;
       $T \leftarrow \text{Append } U \text{ on the candidate tree } T$ ;
    end
    if  $c_l(\mathbf{v}^0) = c'_l$  then
       $t \leftarrow t + 1$ ;
      if  $t = N_{t1}$  then
        break;
      end
    else
       $t \leftarrow 0$ ;
       $c'_l \leftarrow c_l(\mathbf{v}^0)$ ;
    end
     $i \leftarrow i + 1$ ;
  end
end
return  $P, T$ .
```

---

---

**Algorithm 5:** PoolTrainingPrethermalization

---

**Input:**  $\mathbb{S}(N_l)$ ,  $P$ ,  $T$ **begin** $\mathbb{S} \leftarrow \mathbb{S}(N_l);$  $i \leftarrow 1$  $\epsilon'_1 = (i - 1)\epsilon_1/N_{i0};$ **for**  $i \leq N_{i1}$  **do** $\mathbb{U}_s \leftarrow \{\};$ **for**  $|\mathbb{U}_s| < N_{s1}$  **do** $U \leftarrow \mathbf{USampling}(\mathbb{S}, T, \epsilon'_1, \epsilon_2);$  $\mathbb{U}_s \leftarrow \mathbb{U}_s \cup \{U\};$  $j \leftarrow j + 1;$ **end** $\mathbb{U}_n(N_{r1}) \leftarrow \mathbf{SolveProb3}(\mathbb{U}_s, P);$ **foreach**  $U \in \mathbb{U}_n(N_{r1})$  **do** $\theta \leftarrow \mathbf{GetParameters}(U, P);$  $\alpha \leftarrow \mathbf{GetStepSize}(\alpha_0);$  $\theta \leftarrow \theta - \alpha \nabla C(U, \theta);$  $P \leftarrow \mathbf{UpdatePool}(\theta, P);$  $T \leftarrow \text{Append } U \text{ on the candidate tree } T;$ **end** $i \leftarrow i + 1;$ **end** $\mathbb{P}_0 \leftarrow \mathbf{Expand}(P);$ **end****return**  $P$ ,  $T$ .

---

---

**Algorithm 6:** PoolTraining

---

**Input:**  $\mathbb{S}(N_l)$ **begin** $P \leftarrow \text{Construct parameter pool with } \mathbf{0} \text{ initialization};$  $T \leftarrow \{\mathbf{v}^0\};$  $P, T \leftarrow \mathbf{PoolTrainingPrethermalization}(\mathbb{S}(N_l), P, T);$  $P, T \leftarrow \mathbf{PoolTrainingMainProcess}(\mathbb{S}(N_l), P, T);$  $\mathbb{P}_0 \leftarrow \mathbf{Expand}(P);$ **end****return**  $\mathbb{P}_0$ ,  $T$ .

---

---

**Algorithm 7:** AlternateTraining

---

**Input:**  $\mathbb{S}(N_l), \mathbb{P}_0, T$ **begin** $\mathbb{P} \leftarrow \mathbb{P}_0$  $\mathbb{U}_s \leftarrow \{\};$  $U_{best} \leftarrow \text{None};$ **for**  $|\mathbb{U}_s| \leq N_{s2}$  **do** $U \leftarrow \text{USampling}(\mathbb{S}, T, \epsilon_1, \epsilon_2);$  $\mathbb{U}_s \leftarrow \mathbb{U}_s \cup \{U\};$ **end** $i \leftarrow 1;$ **for**  $i \leq N_{i2}$  **do** $\mathbb{U}_n(N_{r2}), \mathbb{U}_n(N'_r), \mathbb{U}_n(N'_r + 1) \leftarrow \text{SolveProb3}(\mathbb{U}_s, \mathbb{P});$ **foreach**  $U \in \mathbb{U}_n(N_{r2})$  **do** $j \leftarrow 1;$ **for**  $j \leq N_o$  **do** $\alpha \leftarrow \text{GetStepSize}(\alpha_0);$  $\theta_U \leftarrow \theta_U - \alpha \nabla C(U, \theta_U);$  $j \leftarrow j + 1;$ **end****end** $\mathbb{U}_{survival} \leftarrow \text{GetSurvivals}(\mathbb{U}_n(N'_r), \mathbb{U}_n(N'_r + 1));$ **if**  $\exists U \in \mathbb{U}_{survival}$  such that  $C(U, \theta_U) < C(U_{best}, \theta_{U_{best}})$  **then** $U_{best} \leftarrow \text{None};$ **end** $\mathbb{U}_{new} \leftarrow \{\};$ **foreach**  $U \in \mathbb{U}_{survival}$  **do** $U_{new} \leftarrow \text{RandomGeneticOperator}(U);$  $\mathbb{U}_{new} \leftarrow \mathbb{U}_{new} \cup \{U_{new}\};$  $\alpha \leftarrow \text{GetStepSize}(\alpha_0);$ **if**  $\alpha \frac{\|\nabla C(U, \theta_U)\|_2}{|\theta_U|} < \xi$  **then** $\mathbb{U}_{survival} \leftarrow \mathbb{U}_{survival} \setminus \{U\};$ **if**  $C(U, \theta_U) < C(U_{best}, \theta_{U_{best}})$  **then** $U_{best} \leftarrow U;$ **end****end****end** $\mathbb{U}_s \leftarrow \mathbb{U}_{survival} \cap \mathbb{U}_{new};$ **for**  $|\mathbb{U}_s| \leq N_{s2}$  **do** $U \leftarrow \text{USampling}(\mathbb{S}, T, \epsilon_1, \epsilon_2);$  $\mathbb{U}_s \leftarrow \mathbb{U}_s \cup \{U\};$ **end****if**  $U_{best}$  has been preserved for  $N_{t2}$  generations **then** $\text{break};$ **end****end** $U^* \leftarrow \arg \min_{U \in \mathbb{U}_s \cup \{U_{best}\}} C(U, \theta_U);$ **end****return**  $U^*, \theta_{U^*}.$ 

---



---

**Algorithm 8:** VQERetraining

---

**Input:**  $U, \theta_0$

**begin**

$\theta \leftarrow \theta_0;$

$i \leftarrow 1$

**for**  $i \leq N_{i3}$  **do**

$\alpha \leftarrow \mathbf{GetStepSize}(\alpha_0);$

$\theta \leftarrow \theta - \alpha \nabla C(U, \theta);$

$i \leftarrow i + 1;$

**if**  $\alpha \frac{\|\nabla C(U, \theta)\|_2}{\|\theta\|} < \xi$  **then**

**break;**

**end**

**end**

$U^* \leftarrow U, \theta^* \leftarrow \theta;$

**end**

**return**  $U^*, \theta^*.$

---